‘This is the peer reviewed version of the following article: Hesp, P. A., Hilton, M., & Konlecher, T. (2017). Flow and sediment transport dynamics in a slot and cauldron blowout and over a foredune, Mason Bay, Stewart Island (Rakiura), NZ. Geomorphology, 295, 598–610. https://doi.org/10.1016/j.geomorph.2017.08.024

which has been published in final form at http://dx.doi.org/10.1016/j.geomorph.2017.08.024

Accepted Manuscript

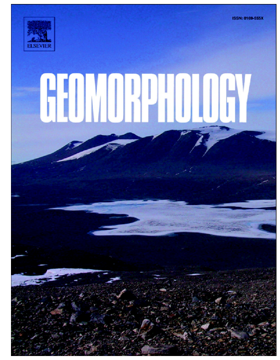

Flow and sediment transport dynamics in a slot and cauldron blowout and over a foredune, Mason Bay, Stewart Island (Rakiura), NZ

Patrick A. Hesp, Michael Hilton, Teresa Konlecher

PII: S0169-555X(17)30328-8
DOI: doi: 10.1016/j.geomorph.2017.08.024
Reference: GEOMOR 6119

To appear in: *Geomorphology*

Received date: 4 April 2017
Revised date: 7 August 2017
Accepted date: 7 August 2017

Please cite this article as: Patrick A. Hesp, Michael Hilton, Teresa Konlecher , Flow and sediment transport dynamics in a slot and cauldron blowout and over a foredune, Mason Bay, Stewart Island (Rakiura), NZ, *Geomorphology* (2017), doi: 10.1016/j.geomorph.2017.08.024

Flow and sediment transport dynamics in a slot and cauldron blowout and over a foredune, Mason Bay, Stewart Island (Rakiura), NZ

Patrick A. Hesp[1], Michael Hilton[2], Teresa Konlecher[3,4]

[1]School of the Environment, Flinders University, Sturt Road, Bedford Park, South Australia 5042.

[2]Department of Geography, University of Otago, P.O Box 56, Dunedin, New Zealand

[3] National Centre for Coasts and Climate, School of Geography, University of Melbourne, Parkville, Victoria 3010

Abstract

This study is the first to simultaneously compare flow and sediment transport through a blowout and over an adjacent foredune, and the first study of flow within a highly sinuous, slot and cauldron blowout. Flow across the foredune transect is similar to that observed in other studies and is primarily modulated by across-dune vegetation density differences. Flow within the blowout is highly complex and exhibits pronounced accelerations and jet flow. It is characterised by marked helicoidal coherent vortices in the mid-regions, and topographically vertically forced flow out of the cauldron portion of the blowout. Instantaneous sediment transport within the blowout is significant compared to transport onto and/or over the adjacent foredune stoss slope and ridge, with the blowout providing a conduit for suspended sediment to reach the downwind foredune upper stoss slope and crest. Medium term (4 months) aeolian sedimentation data indicates sand is accumulating in the blowout entrance while erosion is taking place throughout the majority of the slot, and deposition is occurring downwind of the cauldron on the foredune ridge. The adjacent lower stoss slope of the foredune is accreting while the upper stoss slope is slightly erosional. Longer term (16 months) pot trap data shows that the majority of foredune upper stoss slope and crest accretion occurs via suspended sediment delivery from the blowout, whereas the majority of the suspended sediment arriving to the well-vegetated foredune stoss slope is deposited on the mid-stoss slope. The results of this study indicate one mechanism of how marked alongshore foredune morphological variability evolves due to the role of blowouts in topographically accelerating flow, and delivering significant aeolian sediment downwind to relatively discrete sections of the foredune.

KEYWORDS

Foredune; slot and cauldron blowout; flow dynamics, aeolian sedimentation

1.0 Introduction

Foredune-blowout complexes are common on the coasts of the Earth (Hesp, 2011; Hesp and Walker, 2013). Blowouts may occur irregularly along the foredune or be prolific in some cases (Hesp, 2002; Mir-Gual et al., 2014). On the New Zealand west coasts located in the 'Roaring 40s', large foredunes with multiple, particularly trough blowouts are common (Hilton, 2000; Hesp, 2001; Shepherd and Hesp, 2003). The foredunes are also commonly densely vegetated by the introduced *Ammophila arenaria* (Marram grass) (Hilton et al., 2005; Konlechner, 2016). In the following, we examine the flow and sediment transport in one such foredune-blowout complex at Mason Bay, Stewart Island, New Zealand, in order to examine the relative differences in flow and sedimentation in a slot blowout and adjacent foredune stoss slope and crest in both the very short term (hours) and longer term (months) .

Foredune morphologies range from a collection or field of nebkhas (forming a foredune zone), to symmetrical, very well vegetated, stable, simple ridges, to highly erosional, poorly vegetated asymmetric knobs (Carter, 1988; Hesp, 2002; Hernandez-Calvento et al., 2007; Davidson-Arnott, 2010; Hesp, 2011; Hernandez-Cordero et al., 2015). Blowout morphologies range from pits, elongated notches, troughs and broad basins (Smith 1960; Koster, 1988), cigar-shaped, v-shaped, scooped hollow, cauldron and corridor (Ritchie, 1972), saucer, trough, cup, and bowl (Black, 1951; Cooper, 1958, 1967; Carter et al., 1990; Gares and Nordstrom, 1995; Hesp 2002; Seppala, 2004; Gutiérrez-Elorza et al., 2005; Hugenholtz and Wolfe, 2005, 2006; Wang et al., 2007; Smyth et al., 2011, 2012, 2013, 2014; Mir-Gual et al., 2012, 2013; Ruz and Hesp, 2014; Abhar et al., 2015), and bitten, conical and mixed shapes (Mir-Gual et al., 2014). Blowouts usually have an erosional portion, and a connected depositional lobe which may range from a pronounced arcuate tongue to a low apron (Carter et al., 1990; Barchyn and Hugenholtz, 2013).

Flow over foredunes can be relatively simple if the slopes are simple morphologies and well vegetated. Flow speed-up occurs upslope, speed-down occurs within the canopy, and most sedimentation takes place on the lower stoss slope except in high to very high wind events where more sediment will be transported further upslope and across the dune via suspension and the occurrence of jets (Arens, 1996; Arens et al., 1995; Hesp et al., 2009, 2013). As the foredune topography becomes more complex, and the vegetation cover more variable, the flow becomes more complex, with potentially high local variations in flow acceleration/deceleration, separation, steering and deflection (Arens, 1996; Arens et al., 1995; Walker et al., 2009a, 2009b; Hesp et al., 2009, 2013, 2015; Petersen et al., 2011; Bauer et al., 2015; Hesp and Smyth, 2016).

The flow within blowouts varies according to their morphology and type. Within trough blowouts, winds are accelerated between the steep walls, sometimes resulting in the formation of jets and helicoidal flow (Hesp and Hyde, 1996; Hansen et al., 2009; Smyth et al., 2014; Smyth and Hesp, 2016). Pronounced topographic steering may occur (Hesp and Pringle, 2001). Speed-up occurs up the stoss slope of the depositional lobe, flow divergence and deceleration occurs across the lobe, and flow separation downwind of the lobe (Carter et al., 1990; Gares and Nordstrom, 1995; Hesp and Hyde, 1996; Smyth and Hesp, 2016). In saucer and bowl blowouts, the flow is often very complex with pronounced topographic steering (Smyth et al., 2014, 2017; Hesp and Walker, 2012).

A turbulent separation zone develops in the lee of the upwind erosional wall where wind flow enters the blowout. Toward the centre of the deflation basin, flow may reattach to the base, becoming realigned to the incident wind direction, before accelerating up the downwind slope and over the blowout rim (Jungerius et al., 1981; Gares and Nordstrom, 1995; Wang et al., 2007; Hugenholtz and Wolfe, 2009; Hesp and Walker, 2011; Smyth et al., 2011; 2012; 2013).

To the authors' knowledge there has been no simultaneous study of flow and sediment transport in a blowout and over an adjacent section of foredune with a relatively simple stoss slope topography. In addition, there are no studies that have examined the comparative relationships between short term (a few hours) flow and transport data and relatively longer term (~1-2 year) sediment deposition data over adjacent foredune slopes and a blowout site. This study, therefore aims to investigate the simultaneous flow and sedimentation across a particular slot blowout morphology and adjacent foredune to examine the dynamics operating in the two landform units, and attempt to better understand the variable nature of sedimentation at various scales ranging from minutes to many months.

2.0 Study Site

Mason Bay is on the west coast of Stewart Island, New Zealand, located off the southern tip of the South Island, and is situated at 46° south (Fig. 1) in Rakiura National Park. The regional climate is maritime temperate (Koppen classification: Cfb) with no strong seasonal contrasts, mean annual rainfall is around 1200 mm and mean temperature is 10°C (Konlechner et al., 2014). The prevailing winds are from the west (Fig. 2). Wind speeds can be very high in this section of the lower Roaring 40s, and sand transport threshold velocities (~6 ms^{-1}) are exceeded 43% of the time at Mason Bay (5 years of wind speed and direction data collected by MH at a permanent meteorological station located on the foredune crest).

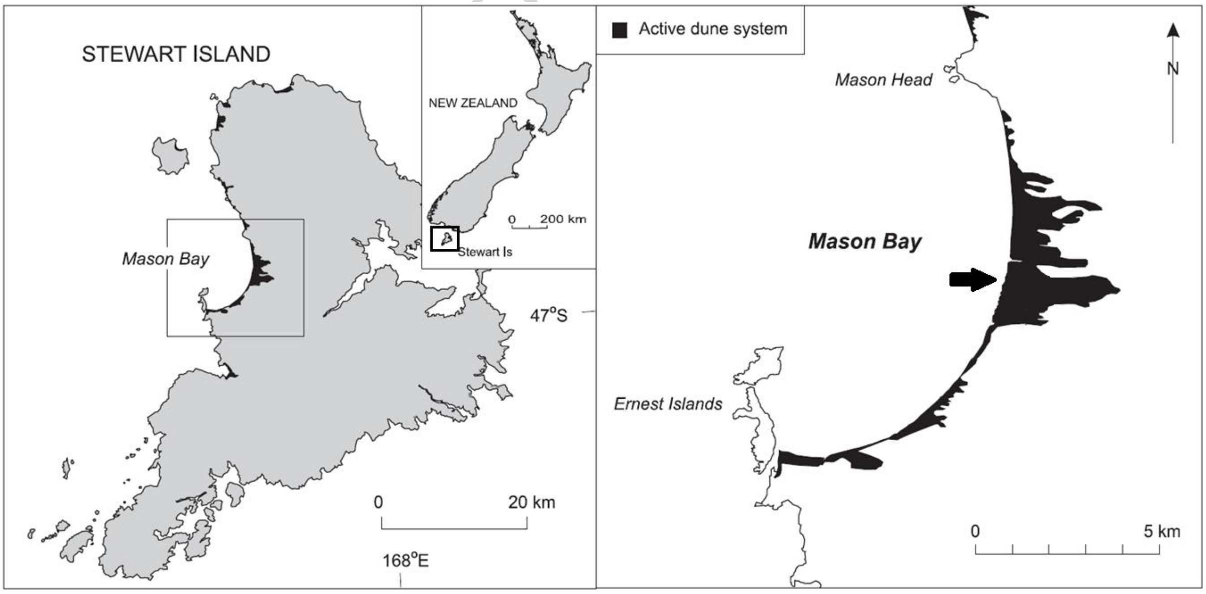

Figure 1: The study site is located at Mason Bay, on the west coast of Stewart Island, New Zealand. The arrow indicates the approximate location of the studied slot and cauldron blowout.

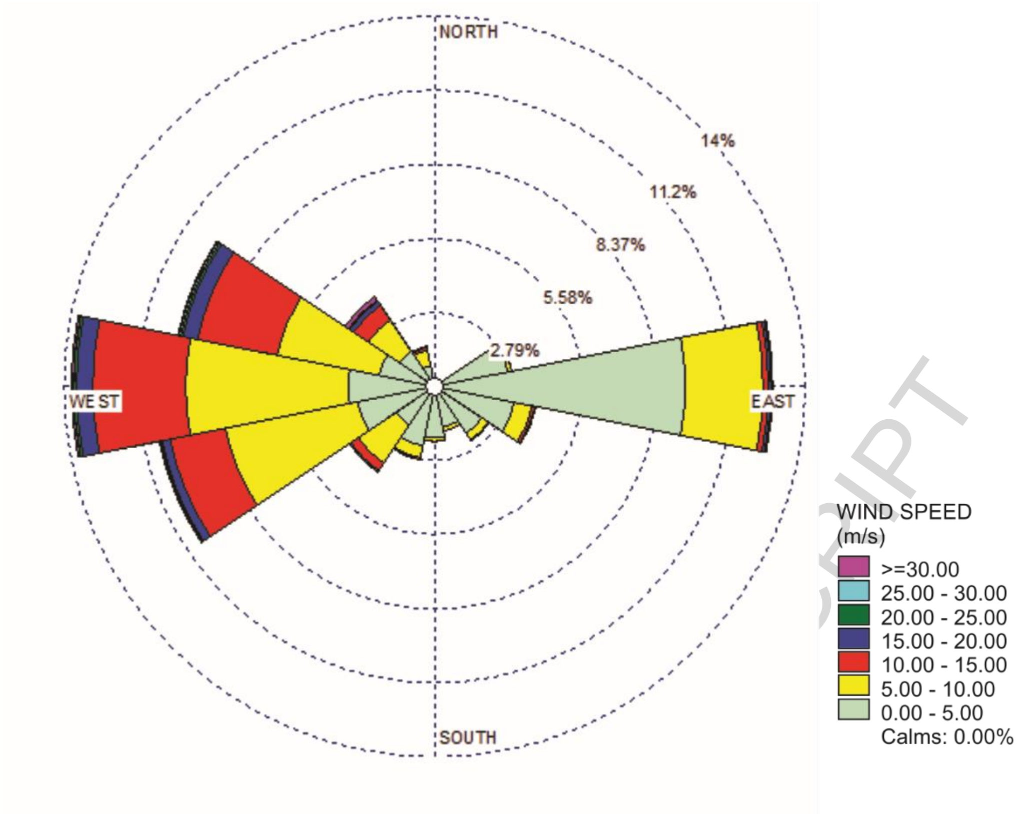

Figure 2: Wind rose for Mason Bay based on 5 years of data (2011-2016) collected on the foredune crest (located in Figure 3).

The coastal dune system has been described by Hilton et al. (2005) and Konlechner et al. (2016), and comprises a large, mixed transgressive and parabolic dunefield barrier (Fig. 3). The seaward margin comprises a well-developed foredune dominated by introduced and invasive *Ammophila arenaria* (marram grass) which colonised the study area in the early 1950's (Hilton et al., 2005; Hart et al., 2012). The foredune prograded about 70 m seawards in the period 1958 to 2003 (Konlechner, 2016), when progradation effectively ceased but the foredune continued to accrete (Petersen et al., 2011). The foredune displays regular flute and ridge topography (or corrugations) in the stoss slope alongshore (Fig. 4) somewhat similar to spur and groove topography on coral reefs.

Figure 3: The dunefield system at Mason Bay, Stewart Island, New Zealand illustrating the foredune-blowout complex with flutes and the location of the slot and cauldron blowout, and then respectively to landwards, parabolic dunes, and transgressive dunefield (including extensive seaward deflation plain). The position of the RM Young anemometer at the permanent meteorological (climate) station is also indicated.

Flutes evolve as a result of the inherent variability in vegetation cover as sand accumulates and ridges form in areas of greater vegetation density, while flutes occur in areas of lower density. Once the initial topographic differences occur, there is positive feedback which acts to increase the height of the ridges relative to the flutes: oblique winds, which are common here, blow sand from the entrance regions of the flutes up onto the ridges thereby increasing the latter's height. At times, some of the flutes are eroded into narrow slot blowouts which resemble pedestrian tracks (Figs. 4, 5). Winds funnel sand into the slots and 'eat' into the landward vegetation and foredune slope carving out bowls and cauldrons at the heads of the slot blowouts. The operation of oblique incident winds also leads to marked topographic steering in the slots and they tend to form curving, upside-down j shapes (ʃ) as they evolve. Seaward progradation of the foredune and lateral spread of dense *Ammophila* vegetation can narrow the slots and increase their total length seawards over time (see Fig. 5).

Figure 4: A portion of the foredune to the south of the study site in 2011. A foredune densely vegetated with *Ammophila* fronts an extensive deflation plain-parabolic and transgressive dunefield complex. Note the regular flute and ridge topography along the stoss slope of the foredune, and the very marked boundary of the crestline indicating the typical landward limit of most aeolian sand deposition (ignoring high wind energy-driven suspension).

This type of flute and ridge corrugated foredune topography is related to the high energy wind environment coupled with the presence of very dense *Ammophila* vegetation cover, and is not seen in regions where the winds and vegetation cover are less. For example, this topography is not at all common on foredunes along the east coast of Australia. Similar foredune topography occurs along the Manawatu coast on the lower North Island of NZ where comparable conditions to Stewart Island occur, i.e. high winds and dense *Ammophila* (Hesp, 2001). There is not a strong seasonal difference in vegetation cover on these foredunes as there is, for example, in higher latitudes. The blowouts that develop at Mason Bay may be similar to those described in Scotland by Ritchie (1972) and termed caldron and corridor blowouts by him.

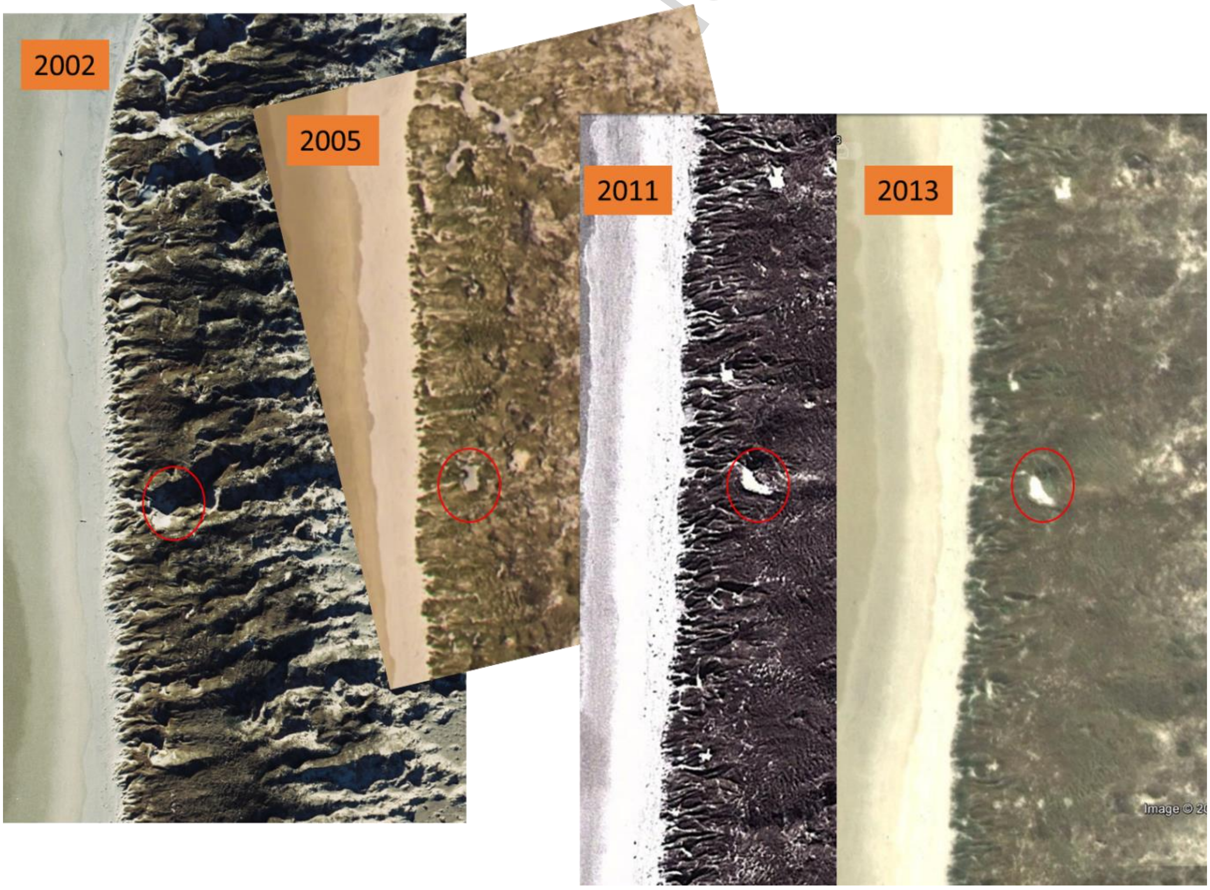

Figure 5: Google Earth images of the experiment slot and cauldron blowout (circled) and adjacent foredune ridge in 2002, 2005, 2011 and 2013. The blowouts were not present in

1989 imagery and largely developed following storm erosion of the foredune prior to 2002. Along the foredune, the slot blowouts are well developed in 2002 and 2011 but are less obvious and more vegetated in 2005 and 2013.

3.0 Methods

The principal aim of the experiment was to examine and compare simultaneous flow and sediment transport through the slot and cauldron blowout and over the adjacent foredune crest. Thus, two rovers comprising four 2-D Windsonic anemometers on each mast were employed to simultaneously gather wind speed and direction data in the blowout and over the foredune. At the conclusion of a run, both anemometer masts were then moved to the next downwind location. This was done in order to be able to directly compare flow dynamics on or within the two different topographies simultaneously. The anemometers were located at 23, 60, 100 and 200 cm above the bed on each rover mast. 10-minute runs were conducted at each location (G1 to G9, and F1 to F9). Thus, for example, in the case of the first run, the G1 (blowout) and F1 (foredune) rovers recorded velocities at exactly the same time at both locations. They were then moved to the second locations (G2 and F2). In order to capture the flow dynamics within the blowout, several rover masts were located within that topographic unit. In addition, in order to determine if sedimentation was occurring across the adjacent foredune upper stoss slope and crest region, rover masts were located at greater distances across that topographic unit. Two permanent Vaissala 2D sonic anemometers were located on the upper backshore, one at 1 m high and one at 2 m height, and 1 m apart. Wind data from the rover masts (indicated as u in the diagrams) were normalised against the mean wind speed at the 2 m mast on the beach (i.e. u/u2000). All sonic anemometers were aligned to magnetic north.

A mast of two vertical, self-orienting sand traps (Hilton et al., 2017) was deployed throughout and across the transects at each rover mast location and across adjacent dunes. The traps were used to trap sand at each rover station when that station was occupied by the roving anemometer masts. That is, the Hilton traps were deployed permanently at each location but were only operated during the time that the rover anemometer mast was at that location. The data are therefore not directly comparable to each other as the traps were not all operating at the same time throughout the experiment. The dense *Ammophila* vegetation was ~55-60 cm high, so trap heights were set at 23 cm and 60 cm above the bed. Semi-permanent pot traps were deployed across the foredune-blowout system at a height just above the foredune vegetation (41–77 cm above the bed). Pot traps are vertical traps designed to collect suspended sand raining down onto the dunes. They consist of a circular, 10 cm diameter plastic pipe attached to a support pole. The pipe is lined with a 63 µm polyester mesh which traps all sand but allows rain to percolate through it.

Fine (0.5 mm diameter) steel erosion pins were placed next to each rover location and left in place for ~4 months to measure net surface elevation change. Miniature, non-recording, high response Windicator 200E wind vanes were deployed at each rover station and at various other points throughout the blowout and across the foredune. The wind directions are monitored via videography and regular compass measurements of mean direction. Colour smoke bombs were deployed at various times in the blowout, during periods of video photography, to assist in visualising 3-D air flow patterns. The incident wind on the beach did not vary much throughout the experiment (Table 1), and the wind direction was remarkably constant (Fig. 6).

Table 1: Variation in incident wind speed and direction derived from a permanently located 2D sonic anemometer located on the upper backshore at 2 m height during the experiment.

	Incident wind speed	Incident wind direction		
	Average (m/s)	Average (°)	Time	duration
	2m	2m		(minutes)
Run1	7.00	239.6	12.40-12.49	9
Run2	7.18	240.9	13.16-13.32	16
Run3	6.73	239.7	13.46-14.00	14
Run4	6.37	241.1	14.15-14.31	16
Run5	5.91	241.6	14.48-15.02	14
Run6	6.66	241.0	15.17-15.34	17
Run7	6.96	246.7	15.50-16.04	14
Run8	6.31	243.2	16.30-16.44	14
Run9	5.94	243.4	17.03-17.17	14

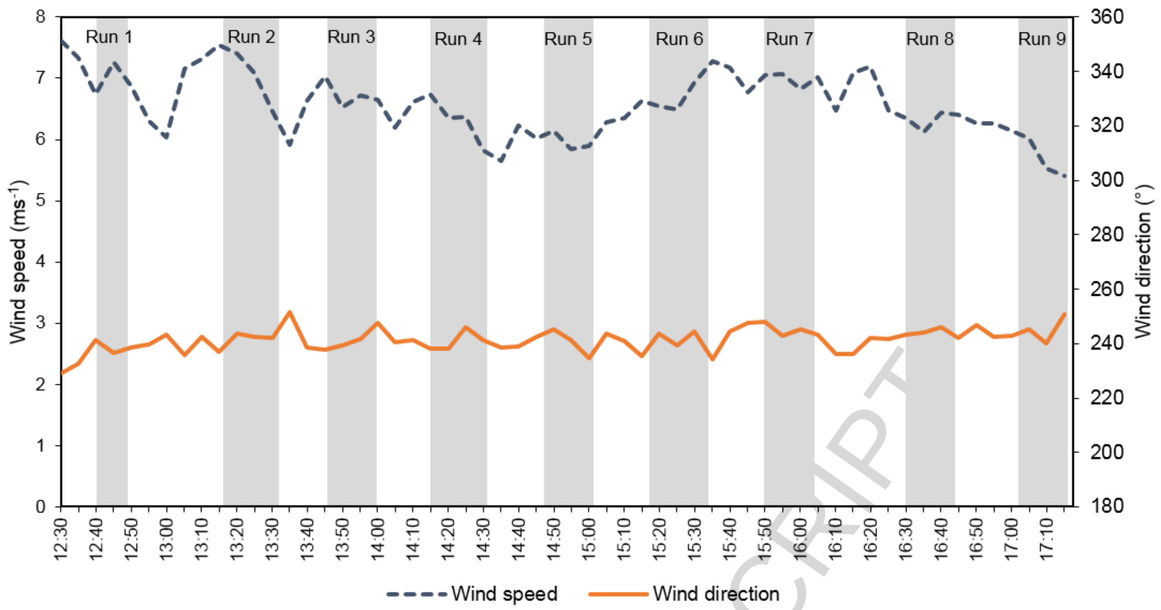

Figure 6: Wind speed and direction recorded at the permanent mast at 2 m height on the backshore. The experimental run periods are indicated by the grey bars.

Figs. 7a and 7b display a contour map of the site and the locations of all permanent and rover masts. The G masts are located through the blowout and beyond, while the F masts are located on an adjacent transect across the foredune.

The beach displayed a dissipative profile and was slightly concave seawards with a gradient of 2°. The exposed beach (above the edge of swash) was ~ 15 m wide at the start of the experiments and the tide continued to fall throughout the experiment.

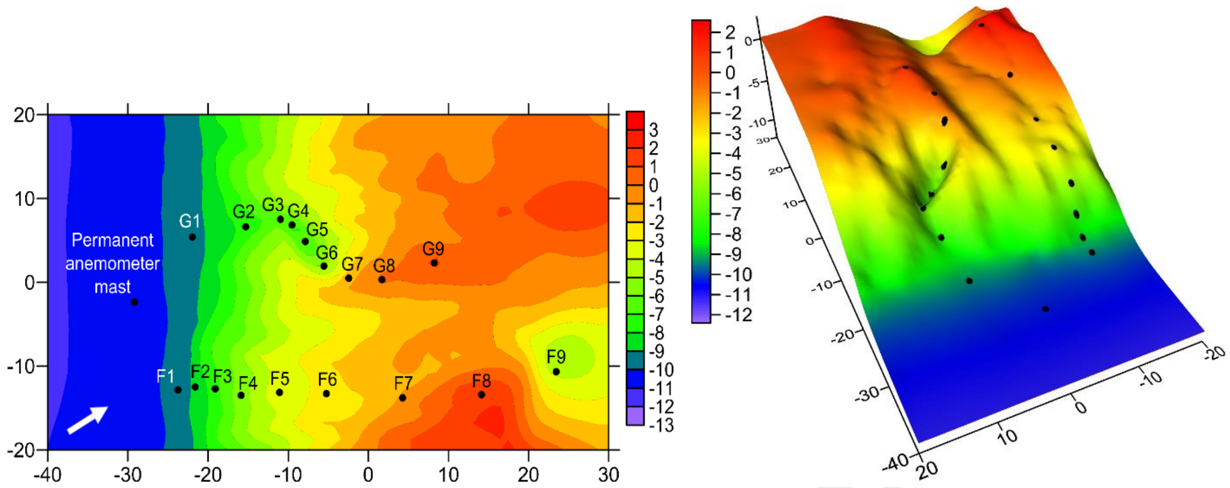

Figure 7a. Location of ultrasonic anemometer masts through the blowout (G1-G9) and across the foredune (F1-F9). Hilton sediment traps were co-located with the masts. The arrow indicates the average wind direction at the 2 m-high permanent mast for the duration of the experiment. Heights are relative to a bench mark situated at an arbitrary 0 m on the foredune crest. 7b: DEM of the study site and locations of the roving anemometer masts and traps.

4.0 Results

4.1 Flow in the slot and cauldron blowout

The flow into and through the slot and cauldron blowout is highly complex. The profile at G1 on the backshore in front of the blowout displays a typical log profile, and maintains this structure while accelerating up the gently inclined backshore into the mouth of the blowout slot to G2. G3 is located just up the seaward portion of the slot on the crest of a small depositional lobe (Figs. 8, 9). The slot at this point is narrow and deep. The velocity profile displays a jet located around 60 to 70 cm above the bed, indicating marked topographic flow compression and acceleration as seen in other trough blowouts (e.g. Hesp and Hyde, 1996).

The mast at G4 was located at the base of the small depositional lobe and around the corner of the slot (see Fig. 7a above). At this location the lowest anemometer is within the plant canopy and the velocity at 23 cm above the bed is markedly reduced. In addition, the three-dimensional wind flow at this location becomes highly turbulent and complex and is characterised by a coherent helicoidal vortex, as observed in other but larger trough blowouts (Hesp and Hyde, 1996). The rotation of this was from right to left looking seawards down the blowout, as observed from multiple videos of smoke bombs (Fig. 10; see additional materials appended to this paper). Thus, the flow above the plant canopy at the G4 location displays a marked deceleration in the 50 to 100 cm height region due to the presence of this vortex. The presence of the helicoidal vortex flow also affects the upper flow structure at G5 half-way up the slot, and the velocity profile is still complex.

Flow near the bed greatly accelerates up the slot. The G6 mast was situated on the top of the mixed depositional deposit-avalanche slope at the base of the cauldron’s vertical scarp (Fig. 9). The wind velocity increases at the lower heights relative to the G5 location as it is accelerated up the avalanche slope. It is clear from the smoke bomb observations and the deflection/steering of the vegetation (Fig. 11) that the flow is vertically accelerated up the scarp wall base. However, at 200 cm high, flow coming over the foredune slope and separating on the leeward slope down into the blowout cauldron creates a complex 3-D flow pattern and the velocity is markedly reduced in the upper portion of the cauldron. G7 was located at the scarp wall crest of the cauldron and is characterised by significant flow acceleration over the scarp. Fig. 11 illustrates how much streamlining and compression of the vegetation takes place at this point.

Above the blowout cauldron, flow is topographically accelerated up the foredune upper stoss-crestal region and percent velocities are 30% greater at 200 cm height above the bed compared to those at the beach. This degree of speed-up is similar to that observed over other foredunes (cf. Arens et al., 1996; Hesp et al., 2009; 2013; Wakes et al., 2010; Petersen et al., 2011; Hesp and Smyth, 2016).

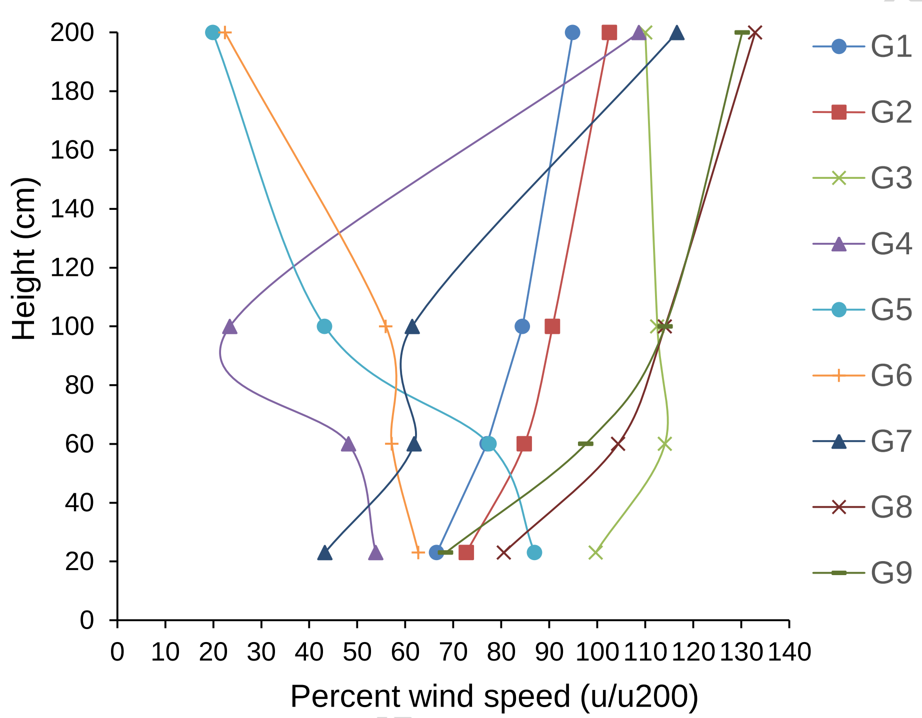

Figure 8: Percent velocity profiles on the backshore and up and over the blowout normalized to a velocity obtained from a permanent UVW station at 200cm height located on the mid-beach (u/u_{200}). G1 is located on the upper backshore, G2 in the blowout entrance, G3-G6 in the blowout slot and cauldron, G7-G9 on the downwind foredune stoss and crest.

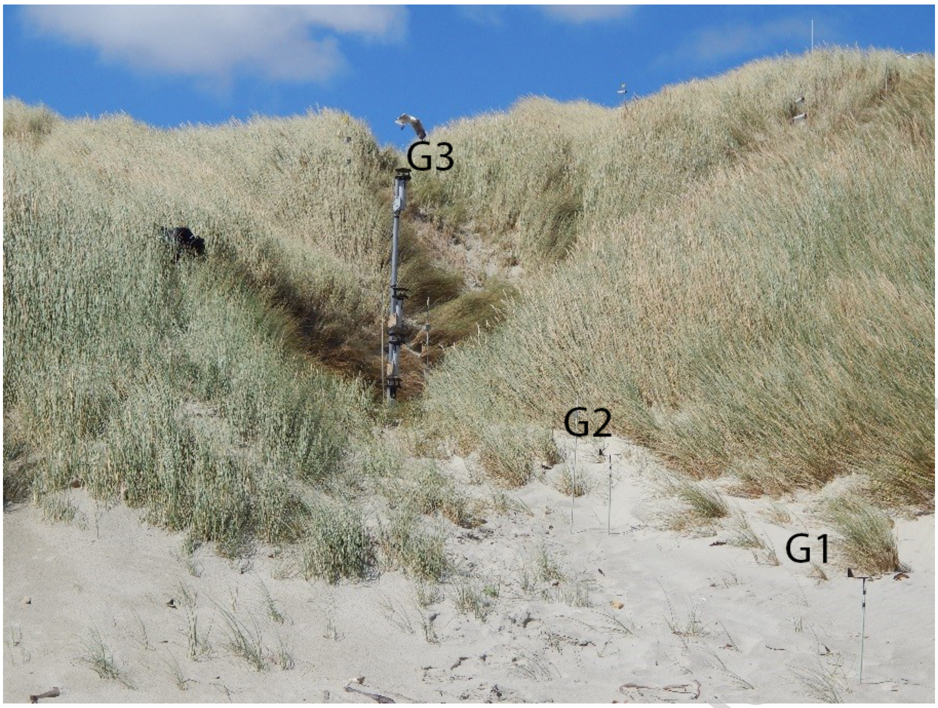

Figure 9: Location of G3 mast in the slot. The position of G1 and G2 is also indicated.

Figure 10. Pictures taken 4 seconds apart of the helicoidal flow operating in the mid-section of the slot blowout. Rotation is from far top left down to bottom right, then upwards and spiralling forwards to the viewer. Note the orientation of the *Ammophila* leaves indicating highly turbulent and directionally variable flow structures.

Figure 11: G6 mast location at the base of the cauldron's vertical scarp, with G5 location indicated in the foreground and Hilton traps also indicated (T). Note the highly complex 3-D flow structure within the slot and cauldron as indicated by the bending directions of the *Ammophila* vegetation.

4.2 Flow over the Foredune

The foredune stoss slope-crest transect is indicated in Figs. 7a and b. The percent cover of vegetation ranged from 40 to 45% in the first 3 metres downwind of the foredune toe, then increased to 60% in the next metre, 70% in the next metre, and thereafter maintained a cover of 80 to 95%.

The mast at F1 displays a similar velocity profile on the upper backshore as G1 (Figs. 12, 13). F2 displays a slightly (5%) lower velocity perhaps due to the proximity of the densely vegetated foredune stoss face. The F3 mast displays a marked reduction in velocity up the entire profile. The first two anemometers are situated well within and at the canopy top (the 23 cm and 60 cm anemometers respectively) and given there is little topographic forcing at this point, the velocities are significantly lower. As the masts were moved progressively up the foredune stoss slope topographic acceleration takes place in the upper flow and increasing drag and deceleration occurs in the lower flow in the vegetation canopy as indicated by F4, F5 and F6 profiles (Figs. 12, 13). These results are nearly identical to those observed by Hesp et al. (2005; 2009) at Prince Edward Island in similar vegetation species, but in lower densities, and similar to those of Arens et al. (2002) The F7 mast was sited in a patch of very dense *Ammophila* and a slight topographic dip and velocities are substantially lower there, despite the fact that it is located higher up the stoss slope. Arens et al. (1995) found similar local and marked variations in wind speed related to local variations in foredune topography. On the foredune crest there is significant speedup again compared to F7 as indicated by the F8 profile, although the flow drag effect of the vegetation on the lower anemometers is obvious. F9 was located in a deep lee dune swale dominated by reversing vortices and displays very low velocities.

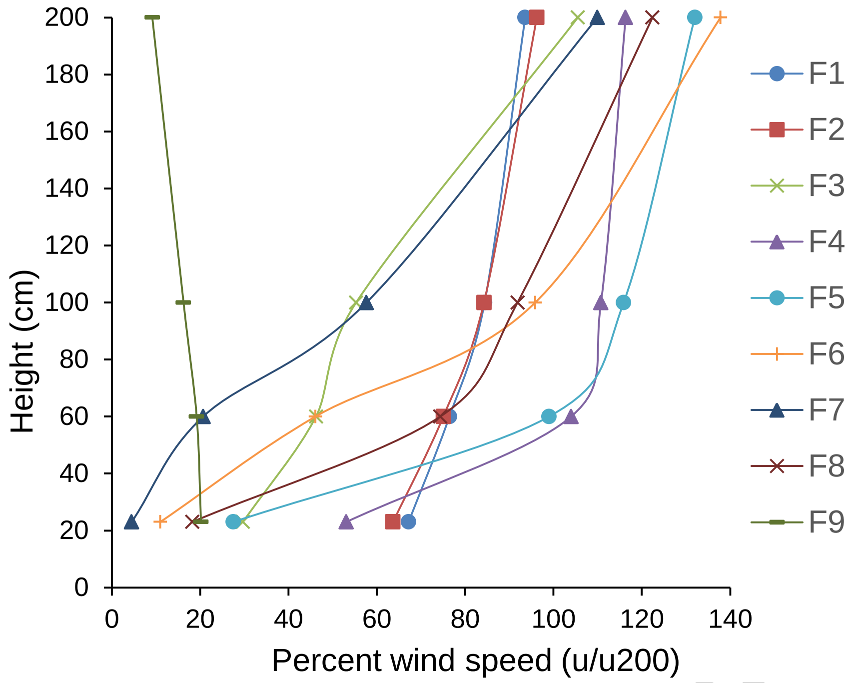

Figure 12: Percent velocity profiles at nine stations across the backshore and foredune adjacent to the blowout, normalized to a velocity obtained from a permanent UVW station at 200cm height located on the mid-beach (u/u_{200}). F1 is on the upper backshore, F2 at the foredune toe, and F3 to F9 located progressively up the foredune stoss slope and crest.

Figure 13: F5 rover mast on the foredune stoss slope transect (crest arrow). The location of the F1 and F2 anemometer masts and sand traps are indicated by the arrows in the foreground.

4.3 Comparison of the blowout and foredune transects.

The percent velocity profiles in front of, and at the entrance of the blowout (G1 and G2) and first two profiles on the foredune transect (F1 and F2) display similar structures but the velocities are lower on the foredune transect (Figs. 8, 12) presumably due to the greater pressure field induced by the foredune compared to the blowout (cf. Wiggs et al., 1996; Walker et al.; 2009; Hesp et al, 2009; 2013; 2015; Hilton et al., 2016). Once in the blowout, the flow markedly increases and a jet is present at G3, whereas on the foredune the presence of the dense *Ammophila* acts to markedly reduce flow velocities within the canopy and immediately above. Speed-up occurs well above the canopy. Further into, and downwind in the blowout, the presence of a marked, coherent helicoidal flow drastically alters the flow field and the velocity profiles are manifestly altered and complex (masts G4, G5 and G6). Further downwind over the foredune, the F4, F5 and F6 profiles display typical speed-down in the vegetation canopy and speed-up above the canopy as the flow is retarded by the vegetation in the lower portion of the profile, and topographically forced across the steep foredune in the upper portion. At the crest of the blowout (G7- uppermost scarp edge of the cauldron) the flow is again high in the upper portion, and the next two profiles (G8 and G9) which are located on the foredune stoss slope and crest are similar to the profiles in comparable locations on the foredune transect (F7, F8).

Clear differences in the flow fields of the two adjacent sites are illustrated in Fig. 14. Here the average flow vectors derived from the sonic anemometer UV velocity data in the blowout and across the foredune for the four sonic anemometer heights at 23, 60, 100 and 200 cm heights are shown. At 23 cm above the bed, there is marked topographic steering and acceleration in the bottom of the blowout, whereas there is mild topographic deflection over the foredune as commonly observed under incident oblique wind conditions (Hesp et al., 2015), and rapid deceleration downwind in the very dense lower *Ammophila* canopy. An examination of the vectors at increasingly higher positions, indicates: (i) that the vectors in the blowout tend to display marked topographic steering aligned by the blowout topography, but are progressively lower in speed with height in the central G5-G6 region; (ii) the vectors over the foredune tend to increase with height above the surface and generally display similar vector directions (except F6 [locally very dense vegetation], and the partial exception of F7); and (iii) the vectors at 200 cm height at G5 and G6 are very low and show the strong influence of the helicoidal vortex operating in that central region of the blowout with vector directions facing offshore and very low velocities.

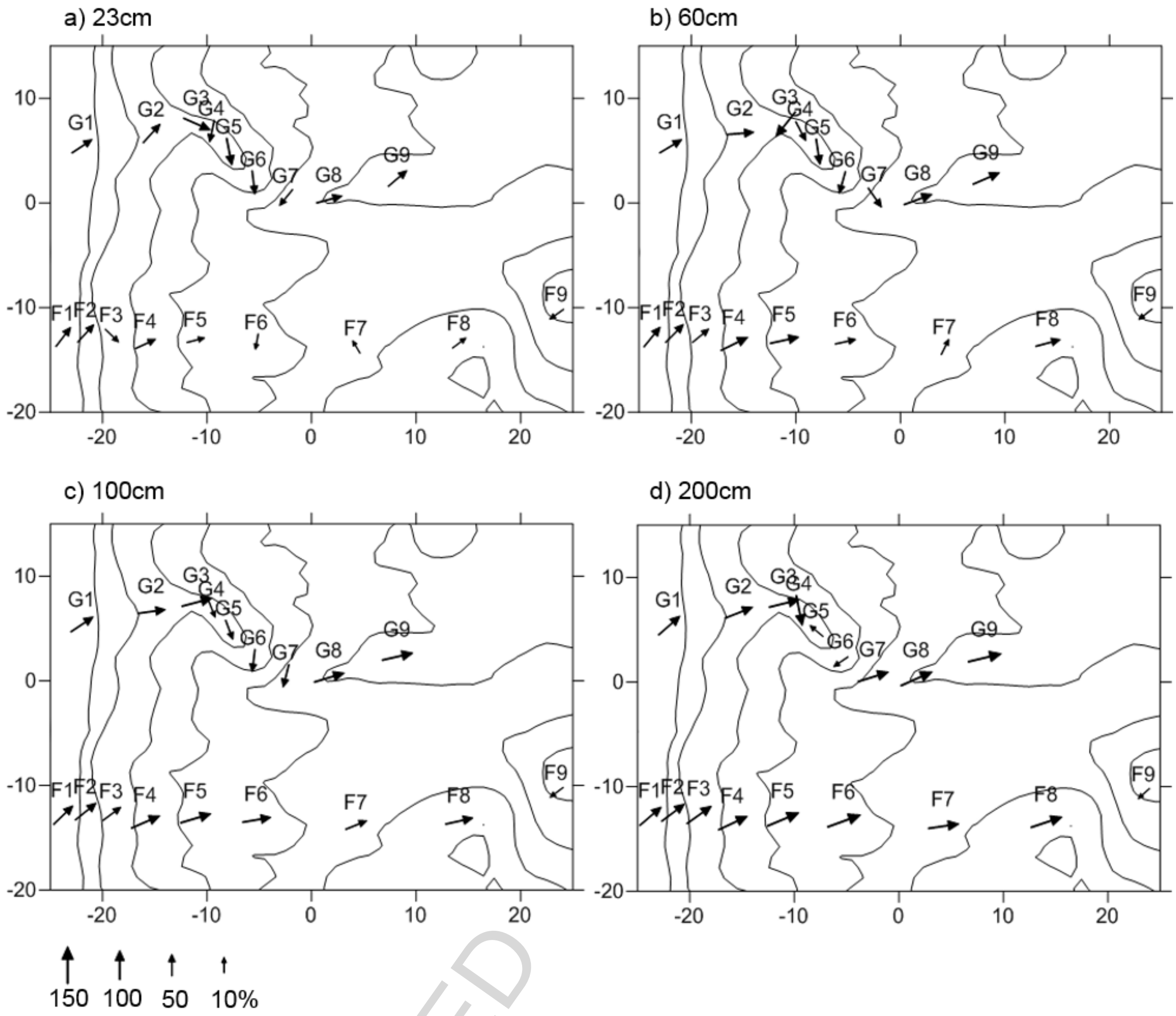

Figure 14: Mean percent flow vectors (velocity [u]/velocity at 200 cm height on the beach sonic) derived from the sonic anemometer UV velocity data in the blowout and across the foredune for the four sonic anemometer heights. Vectors plotted at rover mast locations. Note the marked topographic steering in the blowout, and flow deflection over the foredune transect.

4.5 Sand transport at short, medium and longer relative temporal scales

Sand transport was measured at each velocity measurement station across the foredune (F1 – F9) and up the blowout (G1-G9) just at the time the rover was present, and continuously at one location on the upper backshore throughout the experiment. The data are therefore not directly comparable as trapping did not occur simultaneously throughout the transects. However, the incident wind on the beach did not vary much throughout the experiment (Table 1), and the wind direction was remarkably constant, so the differences between the trap data are not particularly related to variations in incident wind velocity.

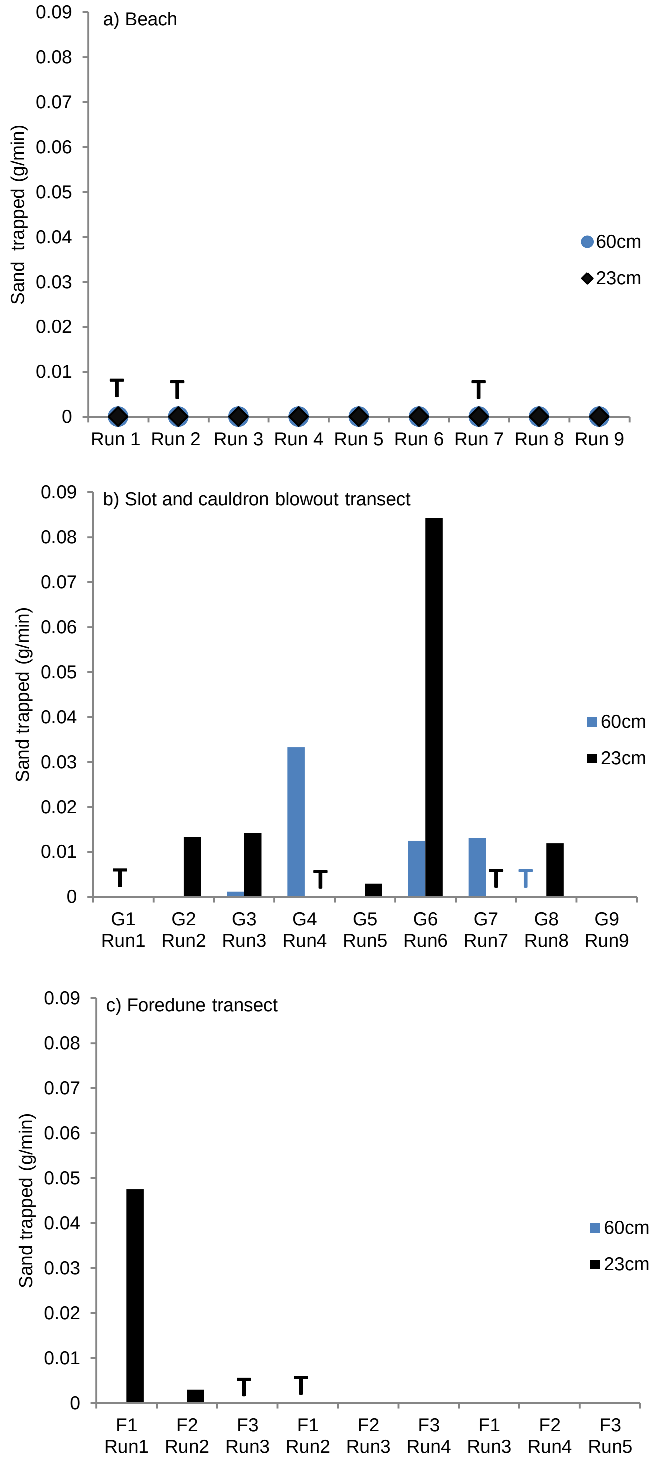

Figure 15: Sand trap data (g/min) collected at each anemometer rover mast location when the rover was present, and at two heights (23 cm and 60 cm). The traps are colour coded and T indicates there was a trace of sand grains collected at the 23 cm (blue) or 60 cm (red) trap height. Sand weighed to 3 decimal places. Run 1 relates to rover positions F1 or G1, Run 2 to F2 or G2 and so on.

The trap data (Fig. 15) show that there was very small (a trace on two occasions) to no transport off the backshore at the location of the beach permanent trap and in front of the blowout (G1) 3 m seawards of the foredune toe, whereas there was significant relative sand trapping on the backshore seawards of the foredune (F1). While there was relatively little sand trapped on the foredune transect at F2 (Run 2) location, and only a trace for the traps located in the vegetation on the lower stoss slope (runs 4, 5; F4 and 5), there was relatively greater trapping throughout the blowout. Sand was moving through the blowout near the bed (trapping at 23 cm high) at G2 (Run 2) and G3 (Run3) whereas at G4 (Run 4) there is significant transport at higher levels due to the highly turbulent helicoidal flow dominating at that point. This occurs because the helicoidal flow here is transporting sand upwards and along the blowout in a swirling motion. High trapping takes place at G6 located at the upper terminus of the avalanche slope/internal ramp located at the base of the caldron scarp (see Fig. 10 for location). Sand is transported in suspension up and over the cauldron scarp and relatively significant amounts of sand are trapped in the dense vegetation on the foredune above the cauldron especially when compared to transport over the foredune transect.

The data shown in Fig. 15 is of course very short term data comprising trapping for 10-15 minutes on one day in relatively moderate (but above threshold) winds. Fig. 16 illustrates longer term (4 months) net surface accretion/erosion data at the rover locations measured with fine erosion pins. The data show that erosion took place just seawards of the foredune toe, and accreted on the lower foredune ridge stoss slope (F3, F4), eroded slightly in the middle stoss slope and accreted up on the crest and immediately in the less of the crest. Sand accreted within the blowout entrance and was eroded throughout the blowout (up to G7). The cauldron scarp wall (G8 at the crest) eroded back while downwind of that, small accretion took place (at G9). These results correlate reasonably well with the short-term observations gathered from the Hilton traps in the blowout, presented above. Most surprising is the small erosion on the upper stoss slope (F6, F7). This is likely related to the presence of lower relative vegetation cover in this location combined with the zone being associated with topographically accelerated wind flow.

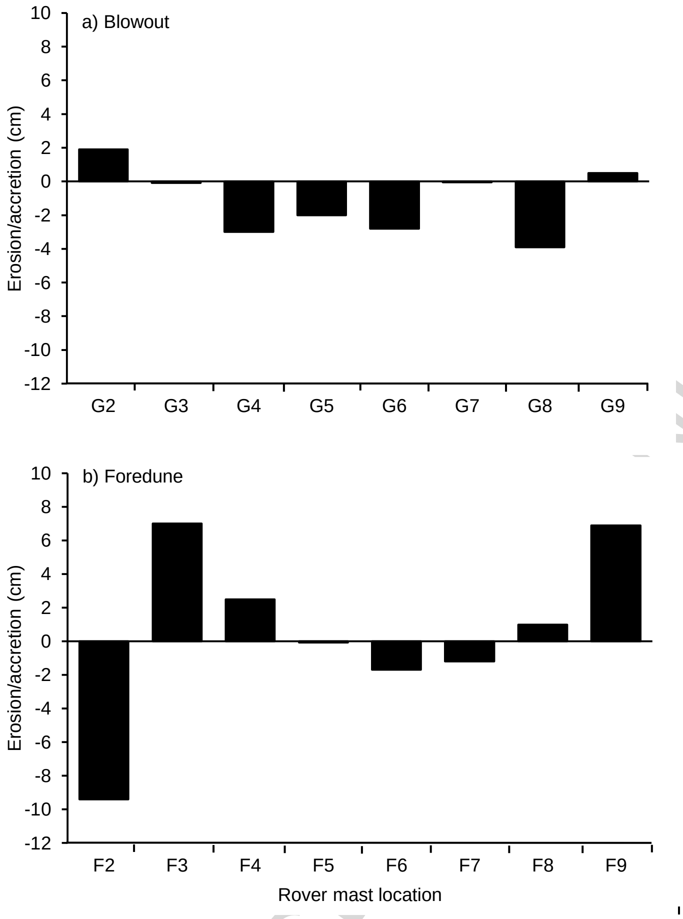

Figure 16. Erosion/accretion (cm) at rover mast locations for the period Jan -Apr 2014. No measurements were made at G1 or F1 on the backshore.

In this region of the lower 'Roaring forties' very significant aeolian sand suspension can take place right across the foredune and downwind (see, for example, Fig. 4 in Hesp, 2011). In order to gain an appreciation of the longer term (months) variable sedimentation patterns via suspension across the foredune-blowout area, pot traps set at 41–77 cm height (Fig. 16a) and which collect only fallout from long-trajectory suspended sedimentation were placed at various locations across the foredune-blowout area (Fig. 17a). The pots were left out for a total period of 16 months and the data are shown in Fig. 17b. Note that Fig. 17b is generated in SURFER software and this software interpolates between sometimes distant points or assigns greater value to outliers than perhaps deserved. Therefore, we have not plotted contours where we do not have a reasonable cover, or any pot trap data in Fig. 17b.

While suspended sediment is delivered to all the foredune-blowout complex from the beach, the pot trap data illustrate the importance of the slot and cauldron blowout in delivering significantly more suspended sediment to the downwind foredune. Fig. 17b shows that there is marked depo-center on the crestal region immediately downwind of the blowout. The amount of deposition is two times that of the highest level recorded on the adjacent foredune crest downwind of the vegetated stoss slope, 600-700 grams of sand deposition (82.4 kg/m^2) compared to 2200-2300+ (27.07 kg/m^2) grams downwind of the blowout. This indicates flow acceleration and topographic steering within the cauldron is resulting in enhanced sedimentation downwind to the foredune crest. Thus, while the blowouts which occur regularly along this foredune remain open to the beach and backshore, the sand moving into the blowout can then be added to that sand eroded from within the blowout and delivered to the landward foredune crestal region.

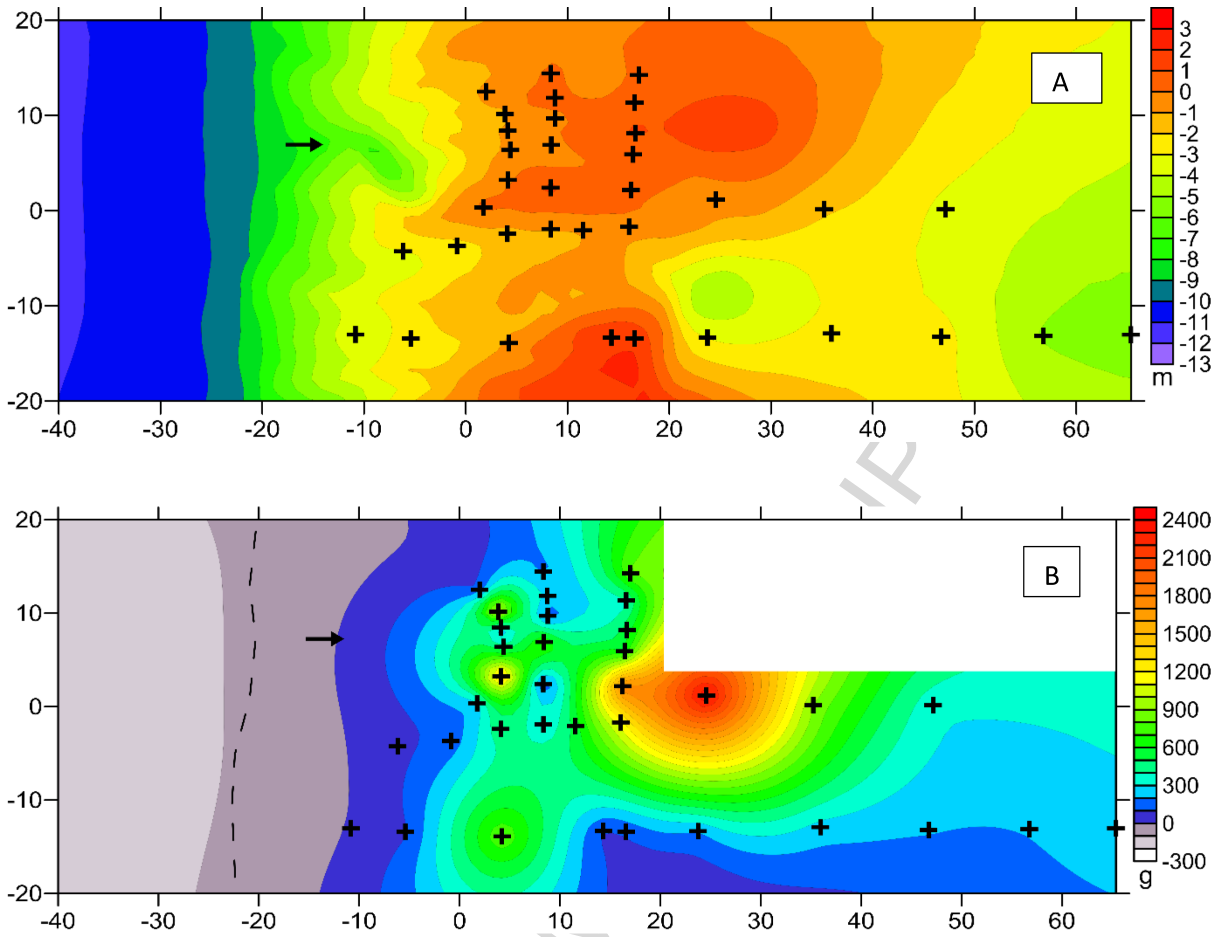

Figure 17: (A) Contour map of the foredune-blowout region and pot trap locations, and (B) contour plot of the pot trap data showing the amount of sand deposited across the foredune via aeolian suspension over a 16 month period (January 2014 – April 2015). The toe of the foredune-limit of the backshore is located approximately at the 9 m contour line in Fig. 17A (identified as the dashed line in Fig. 17B), and the mouth of the slot blowout identified by the arrow in both images. Pot locations are identified by crosses. Significantly greater aeolian sedimentation takes place in the lee of the slot-cauldron blowout compared to the adjacent foredune ridge.

Overall, the very short term sand transport data provided by the Hilton traps operated during the experiment show that considerable sand is moving throughout the blowout, the 4-month data indicate a similar difference between the blowout transect and the adjacent foredune stoss slope, and the relatively longer term 16-months suspension date indicate a significant delivery of sand to the foredune crest downwind of the blowout. The two transects display very different velocity profiles and their 3-D flow structures are quite dissimilar; highly turbulent and with extensive, coherent helicoidal vortices in the blowout versus a simpler almost 2-D flow across the vegetated stoss slope. Coupled together, the flow and erosion/sedimentation patterns in the blowout are markedly different than those across the vegetated stoss slope and crest.

In terms of a comparison with other studies, the flow dynamics over the foredune compare well, i.e. are similar to those observed by, for example, Arens et al. (1995, 2002), Petersen et al. (2011), Walker et al. (2009a, 2009b), Hesp et al. (2009, 2013, 2015), Hesp and Smyth (2016) and Bauer et al. (2015). Flow is accelerated above the plant canopy up stoss slopes, and significantly impeded and reduced within the canopy, with the degree of flow drag strongly controlled by distance downwind, local variations in vegetation density, and local topographic variations. Arens et al. (2002) found that suspended sediment transport was far more important than saltation on densely vegetated foredunes as this study also shows. In a single, relatively high velocity wind event, Arens et al. (2002) found that transport volumes were 1000 times less over the foredune compared to those occurring on the beach. In this present study, the longer term pot trap data demonstrates that significant amounts of suspended sand can be delivered to the foredune upper stoss slope and crest. In addition, significantly greater volumes of sediment are locally delivered to the foredune crest via transport from the blowout.

5.0 Conclusions

The following conclusions may be made:

This study is the first study to the authors' knowledge simultaneously comparing flow and sediment transport through a blowout and over an adjacent foredune, and the first study of flow within a highly sinuous, slot and cauldron blowout;

Flow across the foredune transect is similar to that observed in other studies (marked flow speed-up over the vegetation and upslope; marked speed-down within the canopy), and is primarily modulated by dune topography, across-dune vegetation density differences, and high to very high plant density, height, and cover compared to other sites;

Flow within the blowout is complex due to the fact that the slot portion of the blowout curves southwards behind the lower foredune stoss slope, and flow separation occurs over the foredune slope into the blowout and interacts with the within-blowout flow. Flow within the blowout exhibits pronounced accelerations and jet flow, is characterised by marked helicoidal coherent flow in the mid-regions, and topographically vertical forced flow out of the cauldron portion of the blowout;

Sediment transport within the blowout is significant compared to transport onto and/or over the adjacent foredune stoss slope and ridge, with the blowout providing a conduit for suspended sediment to reach the foredune upper stoss slope and crest, at times when the adjacent foredune stoss slope and crest is largely inactive, or sedimentation is confined to the lowermost stoss face;

Medium-term (4 months) aeolian sedimentation data indicates sand is accumulating in the blowout entrance while erosion is taking place throughout the majority of the slot, and deposition is occurring downwind of the cauldron on the downwind foredune ridge. The adjacent lower stoss slope of the foredune is accreting while the upper stoss slope is slightly erosional;

Longer term (16 months) pot trap data shows that the majority of foredune upper stoss slope and crest accretion occurs via suspended sediment delivery from the blowout. Whereas the majority of the suspended sediment arriving to the foredune stoss slope is deposited on the mid-stoss slope;

The results of this study illustrate one mechanism of how alongshore foredune morphological variability occurs. Blowouts erode and the flow escaping the blowout delivers that eroded sand downwind to the foredune crest and beyond, building the blowout depositional lobe and also the foredune crest higher. On sections of well vegetated foredunes without blowouts, lower stoss slope accretion is dominant where sand is delivered via saltation, and mid-stoss slope accretion is likely dominant where sand is delivered by suspension (cf. Hesp, 1988; Arens et al., 1995; Arens, 1996; Hesp, et al., 2013).

Acknowledgements

Patrick Hesp thanks Flinders University for support. The authors are grateful for the support of the Department of Conservation (Rakiura National Park), the University of Otago, and the Department of Geography, University of Otago. Thanks to Robin Davidson-Arnott, an anonymous reviewer and the editor, Andrew Plater for their critiques of the paper and assistance in improving it.

References

Abhar, K.C., Walker, I.J., Hesp, P.A., Gares, P.A., 2015. Spatial-temporal evolution of aeolian blowout dunes at Cape Cod. Geomorphology 236, 148-162.

Arens, S. M., 1996. Patterns of sand transport on vegetated foredunes. Geomorphology, 17(4), 339-350.

Arens, S.M., van Kaam-Peters, H.M.E., van Boxel, J.H., 1995. Air flow over foredunes and implications for sand transport. Earth Surface Processes and Landforms 20, 315–332.

Barchyn, T.E., Hugenholtz, C.H., 2013. Dune field reactivation from blowouts: Sevier Desert, UT, USA. Aeolian Research 11, 75-84, doi:10.1016/j.aeolia.2013.08.003

Bauer, B.O., Hesp, P.A., Walker, I.J., Davidson-Arnott, R.G.D., 2015. Sediment (dis)continuity across a beach-dune profile during an offshore wind event. Geomorphology 245, 135-148.

Black, R.F., 1951. Eolian deposits of Alaska. Arctic 4 (2), 89–111. doi: 10.14430/arctic3938

Carter, R.W.G., 1988. Coastal Environments. Academic Press.

Carter, R.W.G., Hesp, P.A., Nordstrom, K.F., 1990. Erosional landforms in coastal dunes. In: Nordstrom, K.F., Psuty, N.P., Carter, R.W.G. (Eds.), Coastal dunes: form and process. Chichester: Wiley, pp. 217– 249.

Cooper, W.S., 1958. Coastal Sand Dunes of Oregon and Washington. Geological Society of America - Memoir 72, 169 pp.

Cooper, W.S., 1967. Coastal Dunes of California. Geological Society of America, Memoir 104, 131 pp.

Davidson-Arnott, R., 2010. Introduction to Coastal Processes and Geomorphology. Cambridge, 442pp.

Gares, P.A., 1992. Topographic changes associated with coastal dune blowouts at island beach State Park, NJ. Earth Surface Processes and Landforms 17(6), 589–604, doi. 10.1002/esp.3290170605..

Gutiérrez-Elorza, M., Desir, G., Gutiérrez-Santolalla, F., Marín, C. 2005.Origin and evolution of playas and blowouts in the semiarid zone of Tierra de Pinares (Duero Basin, Spain).Geomorphology, 72(1-4), pp.177–192.

Hack, J., 1941. Dunes of the western Navajo Country. Geographical Review, 31(2): 240-264.

Hart, A. T., Hilton, M. J., Wakes, S. J., Dickinson, K. J., 2012. The impact of Ammophila arenaria foredune development on downwind aerodynamics and parabolic dune development. Journal of Coastal Research, 28(1), 112-122.

Hernández-Calvento, L., Alonso, I., Sánchez-Pérez, I., Alcántara-Carrió, J., Montesdeoca, I., 2007. Shortage of sediments in the Maspalomas dune field (Gran Canaria, Canary Islands) deduced from analysis of aerial photographs, foraminiferal content, and sediment transport trends. Journal of Coastal Research, July, 993-999.

Hernández-Cordero, A. I., Pérez-Chacón Espino, E., Hernández-Calvento, L., 2015. Vegetation, distance to the coast, and aeolian geomorphic processes and landforms in a transgressive arid coastal dune system. Physical Geography, 36(1), 60-83.

Hesp, P.A., 1988. Morphology, dynamics and internal stratification of some established foredunes in southeast Australia. Sedimentary Geology 55, 17-41.

Hesp, P.A., 2001; The Manawatu dunefield: Environmental change and human impacts. NZ Geographer 57 (2), 41-47.

Hesp, P.A., 2002. Foredunes and Blowouts: initiation, geomorphology and dynamics. Geomorphology 48, 245-268.

Hesp P.A., 2011. Dune coasts. In: Wolanski E and McLusky DS (eds.) Treatise on Estuarine and Coastal Science, Vol 3, Waltham: Academic Press, 193–221.

Hesp, P.A**.,** Hyde, R., 1996; Flow dynamics and geomorphology of a trough blowout. Sedimentology 43, 505-525.

Hesp, P.A., Pringle, A., 2001; Wind flow and topographic steering within a trough blowout. J. Coastal Research Special Issue 34, 597-601.

Hesp, P.A. Smyth, T.A.G., 2016. Jet flow over foredunes. Earth Surface Processes and Landforms 41, 1727-1735. DOI: 10.1002/esp.3945

Hesp, P.A., Smyth, T.A.G., Nielsen, P., Walker, I.J., Bauer, B.O., Davidson-Arnott, R.G., 2015. Flow deflection over a foredune. Geomorphology 230, 64-74.

Hesp, P. A., Walker, I.J., 2012. Three-dimensional æolian dynamics within a bowl blowout during offshore winds: Greenwich Dunes, Prince Edward Island, Canada. Aeolian Research 3, 389–399, doi:10.1016/j.aeolia.2011.09.002

Hesp, P.A., Walker, I.J., 2013. Aeolian environments: coastal dunes. In: Shroder, J. (Editor in Chief), Lancaster, N., Sherman, D.J., Baas, A.C.W. (Eds.), Treatise on Geomorphology, vol. 11, Aeolian Geomorphology. Academic Press, San Diego, CA, pp. 109-133.

Hesp, P.A**.,** Walker, I.J., Chapman, C., Davidson-Arnott, R., Bauer, B.O., 2013. Æolian dynamics over a foredune, Prince Edward Island, Canada. Earth Surface Processes and Landforms 38 (1), 1566–1575. doi: 10.1002/esp.3444

Hesp, P.A., I.J. Walker, S.L. Namikas, R. Davidson-Arnott, B.O. Bauer, Ollerhead, J., 2009. Storm wind flow over a foredune, Prince Edward Island, Canada. J. Coastal Research SI 56, 312-316.

Hilton, M.; Duncan. M., Jul, A., 2005. Processes of *Ammophila arenaria* (Marram Grass) invasion and indigenous species displacement, Stewart Island, New Zealand. Journal of Coastal Research, 21(1), 175-185.

Hilton, M., Nickling, B., Wakes, S., Sherman, D., Konlechner, T.M., Jermy, M., Geoghegan, P., 2017. An efficient, self-orienting, vertical-array, sand trap. Aeolian Research, 25, 11-21.

Hugenholtz, C., Wolfe, S., 2005. Biogeomorphic model of dunefield activation and stabilization on the northern Great Plains. Geomorphology 70(1-2), 53-70, doi. 10.1016/j.geomorph.2005.03.011

Hugenholtz, C.H., Wolfe, S.A., 2006.Morphodynamics and climate controls of two aeolian blowouts on the northern Great Plains , Canada. Earth Surface Processes and Landforms 31(12),1540-1557, doi:10.1002/esp.1367).

Jungerius, P.D., Verheggen, A.J., Wiggers, A.J., 1981. The development of blowouts in ‘De Blink’, a coastal dune area near Noordwijkerhout, The Netherlands. Earth Surface Processes and Landforms 6 (3-4), 375–396. doi. 10.1002/esp.3290060316

Konlechner. T,M., Hilton, M.J., Arens, S.M., 2014. Transgressive dune development following deliberate de-vegetation for dune restoration in the Netherlands and New Zealand. Dynamic Environments, 33, 141-154.

Konlechner, T. M., Buckley, E. E., Hilton, M. J., Wakes, S. J., 2016. Downwind dune dynamics following *Ammophila arenaria* invasion. Journal of Coastal Research, SI 75, 298-302.

Koster, E.A., 1988. Ancient and modern cold climate aeolian sand deposition: a review. J. Quaternary Science 3 (1), 69-83.

Mir-Gual, M. Pons, G.X., Gelabert, B., Martin-Prieto, J.A., Rodríguez-Perea. A., 2014. Conservation approach of a front dune system through the study of its blowouts (cala Agulla, Mallorca). Boll. Soc. Hist. Nat. Balears 57, 79-103.

Mir-Gual, M. Pons, G.X., Martin-Prieto, J.A., Roig-Munar, F.X., Rodríguez-Perea. A., 2012. Geomorphological and ecological features of blowouts in a western Mediterranean coastal dune complex: a case study of the Es Comú de Muro beach-dune system on the island of Mallorca, Spain. Geo-Marine Letters, 33(2-3),129-141. doi:10.1007/s00367-012-0289-7

Petersen, P. S., Hilton, M. J., Wakes, S. J., 2011. Evidence of aeolian sediment transport across an Ammophila arenaria-dominated foredune, Mason Bay, Stewart Island. New Zealand Geographer 67 (3), 174-189.

Ritchie, W. 1972. The evolution of coastal sand dunes. Scottish Geographical Magazine 88, 19-35. doi: 10.1080/00369227208736205

Ruz, M-H., Hesp, P.A., 2014. Geomorphology of high latitude coastal dunes, In: Martini, I.P. and Wanless, H.R. (eds), Sedimentary Coastal Zones from High to Low Latitudes: Similarities and Differences. The Geological Society London, Special Publication pp. 388: 199-212, doi:10.1144/SP388.17

Seppala, M., 2004. Wind as a Geomorphic Agent in Cold Climates. Cambridge Univ. Press, 358pp.

Shepherd, M.J. and Hesp, P.A., 2003. New Zealand coastal barriers and dunes. Chpt. 8 *In:* H. Rouse, J. Goff and S. Nichol (Editors), The New Zealand Coast: Te Tai O Aoteoroa. Dunmore Press in assoc. with Whitireia Publishing and Daphne Brasell Associates Ltd., Palmerston North, NZ, 163-190.

Smith, A., Gares, P., Wasklewicz, T., Hesp, P.A., Walker, I.J., 2017 (in press). Short-term morphologic changes of a bowl blowout, Cape Cod , USA. Geomorphology.

Smith, H.T.U., 1960. Physiography and photo interpretation of coastal sand dunes. Final Report Contract NONR - 2242(00), Office of Naval Research, Geographical Branch, 60 pp.

Smyth, T.A.G., Hesp. P.A., 2016. CFD modelling of turbulent flow structures in a trough blowout. J. Coastal Research S.I. 75, 328-332.

Smyth, T.A.G., Jackson, D.W.T., Cooper, J.A.G., 2011. Computational fluid dynamic modelling of three-dimensional airflow over dune blowouts. Journal of Coastal Research, 64, 314–318. doi:10.1016/j.geomorph.2012.07.014

Smyth, T.A.G., Jackson, D.W.T., Cooper, J.A.G., 2012. High resolution measured and modelled three-dimensional airflow over a coastal bowl blowout. Geomorphology 177-178, 62-73, doi:10.1016/j.geomorph.2012.07.014

Smyth, T.A.G., Jackson, D.W.T., Cooper, J.A.G., 2013. Three dimensional airflow patterns within a coastal blowout during fresh breeze to hurricane force winds. Aeolian Research, 9, 111 – 123, doi:10.1016/j.geomorph.2012.07.014

Smyth, T.A.G., Jackson, D.W.T., Cooper, J.A.G., 2014. Airflow and aeolian sediment transport patterns within a coastal trough blowout during lateral wind conditions, Earth Surface Processes and Landforms 39(14),1847-1854., doi: 10.1002/esp.3572

Wakes, S. J., Maegli, T., Dickinson, K. J., Hilton, M. J., 2010. Numerical modelling of wind flow over a complex topography. Environmental Modelling & Software, 25(2), 237-247.

Walker, I.J., Davidson-Arnott, R.G.D., Hesp, P.A., Bauer, B.O., Ollerhead, J., 2009a. Mean flow and turbulence responses in airflow over foredunes: new insights from recent research. J. Coastal Research SI 56, 366-370.

Walker, I.J., Hesp, P.A., Davidson-Arnott, R.G.D., Bauer, B.O., Namikas, S.L., Ollerhead, J., 2009b. Responses of 3-D flow to variations in the angle of incident wind and profile form of dunes: Greenwich Dunes, Prince Edward Island, Canada. Geomorphology 105 (1-2), 127-138.

Wang Shuai, Hasi Eerdun, Zhang Jun and Zhang Ping, 2007. Geomorphological significance of air flow over a saucer blowout of the Hulun Buir sandy grassland. Journal of Desert Research 27(5), 745–749.